BNL-224607-2023-COPA

Modeling Adequacy of Droop-Controlled Grid-Forming Converters for Transient Studies: Singular Perturbation Analysis

A. Yogarathnam

Submitted to the 2023 Institute of Electrical and Electronics Engineers (IEEE) Power & Energy Society Innovative Smart Grid Technologies (ISGT) Conference
to be held at Washington, DC, USA
January 16 - 19, 2023

Interdisciplinary Science Department

Brookhaven National Laboratory

U.S. Department of Energy

USDOE Office of Electricity Delivery and Energy Reliability (OE), Power Systems Engineering Research and Development (OE-10)

DISCLAIMER

Modeling Adequacy of Droop-Controlled Grid-Forming Converters for Transient Studies: Singular Perturbation Analysis

[1]Amirthagunaraj Yogarathnam,[2]Lilan Karunaratne [2]Nilanjan Ray Chaudhuri, and [1]Meng Yue
[1]*Interdisciplinary Science Department*, Brookhaven National Laboratory, Upton, NY, USA
[2]*School of Electrical Engineering and Computer Science*, Pennsylvania State University, University Park, PA, USA
emails: ayogarath@bnl.gov, lvk5363@psu.edu, nuc88@psu.edu, yuemeng@bnl.gov

***Abstract*—The converter-interfaced generation (CIGs) are expected to dominate the grid of the future. These CIGs will cohabit with a small percentage of synchronous generators (SGs) producing power from hydro, solar thermal or even nuclear resources. It appears that the literature lacks comprehensive modeling adequacy studies on such grids with SGs and CIGs. This paper takes the first step in that direction. To that end, a nonlinear averaged phasor model of the system with detailed model of the converters including grid-forming converters (GFCs) and their control is developed. Then a singular perturbation analysis based model reduction approach for such system is proposed. Based on the proposed method, two levels of reduced order models for the GFCs are derived. Finally, the adequacy of these reduced-order models are presented via time-domain simulations on two test system models using MATLAB/Simulink.**

***Index Terms*—Grid-forming converter, droop-control, dc current limit, singular perturbation analysis, model reduction.**

I. Introduction

The present-day grid is dominated by a declining fleet of synchronous generators (SGs) with increasing penetration of converter-interfaced generation (CIG) technology. The grid of the future is expected to be dominated by CIGs, which will cohabit with a small percentage of SGs producing power from hydro, solar thermal or even nuclear resources. A comprehensive understanding of the dynamics of such systems is crucial for planning and operation of the power systems. The CIGs introduce dynamics of different time-scales than traditional SGs and their associated controls. Typically, differential algebraic equations (DAEs) are used to represent such power system models that can easily reach thousands of equations, even for a moderately large system. Simulation of these models, particularly for large-scale system with detailed electromagnetic transient (EMT) models of converters, for dynamic analysis becomes a computationally challenging task, especially due to a wide range of time-scales involved.

A significant amount of literature exists that has studied the impact of high penetration of CIGs in bulk power grids with progressively declining inertia and its impact on system stability [1]–[4]. Most of the research, however, has only focused on "use-cases" based upon either time- or frequency-domain analysis. These use-cases, although valuable, are mostly numerical in nature and draw conclusions dependent on system configurations and loading conditions. Moreover, since the CIGs are typically based on grid-following converters (GFLCs), most studies have considered this technology. Furthermore, these studies have assumed a varying degree of fidelity of CIG models and considered that the traditional fundamental frequency phasor models that neglect transmission line dynamics are adequate for such studies.

Although significant work has been done on modeling of microgrids (e.g., [5]–[7]) and grids with 100% CIGs (e.g. [8]–[11]), few studies exist on developing a modeling framework for the grid of our interest that can be analytically justified to meet the requirement of capturing frequency dynamics in the grid under transition. On the other hand, extensive research including [12] has been reported on determining modeling adequacy in traditional grids with SGs, to the best of our knowledge, there exist a few papers that have performed similar analysis on grids with both SGs and CIGs. Singular perturbation theory was applied in [13] for model reduction of a system with a single converter connected to an infinite bus.

In [14], singular perturbation analysis was performed for nonlinear models with SGs and CIGs, which did not take the control loops into account. Reference [15] presented the effect of transmission line dynamics in a couple of test systems with SGs, grid-forming converters (GFCs), and GFLCs through numerical analysis of the linearized models. It was shown in [15] that network dynamics introduces both positive and negative effects on stability in systems with GFCs and SGs. A recent paper [16] applied singular perturbation theory on the modeling adequacy study of grids with GFLCs.

In a recent work [11], the authors pointed out deficiencies of the existing literature and summarized the major challenges of low-inertia systems where SGs, and GFCs coexist. Out of these challenges, one important area is primary frequency response following loss of an SG. To develop understanding of the timescale separation present between GFCs and SGs in the context of frequency dynamics, an analytical approach has to be developed to establish modeling adequacy of such systems. This will in turn help reduce the models, while retaining the dynamics of interest. It appears that the literature lacks

This study is supported by the Advanced Grid Modeling (AGM) Program of the Office of Electricity, the Department of Energy (DOE).

comprehensive modeling adequacy studies on grids with SGs and GFCs. This paper takes the first step in that direction.

The paper is organized as follows: Section II presents the details power system models and controls. In Section III, the proposed singular perturbation analysis is discussed. Section IV presents case studies on two test systems with a GFC. Section V summarizes this study and identifies the future work.

II. Nonlinear State-Space Model of the System

In this study, a positive sequence fundamental frequency phasor models for representing the test systems is considered. A brief description each of the components are described below.

SG Model: The SGs are represented using either a classical model or an 8^{th}-order model in an orthogonal d-q reference frame rotating at the same speed as that of the machine's rotor [17]. The stator transients are represented using the stator fluxes as state variables.

Exciter Model: The 8^{th}-order SG models are also modeled with an IEEE-DC1A type exciter [17].

Load Model: The loads in the system are modeled as constant impedance, constant current, or constant power load or combinations of them.

AC Network Model: The transformers and transmission lines in this system are modeled algebraically. The AC network is modeled algebraically using a Y -bus matrix in a current injection framework.

The detailed modeling of GFC is discussed next.

A. Grid-Forming Converter and Controls

In this paper, we considered the voltage-sourced converters (VSCs) as the power processors for the GFCs. As shown in Fig. 1, the averaged model of GFCs is represented in a $d-q$ frame [18].

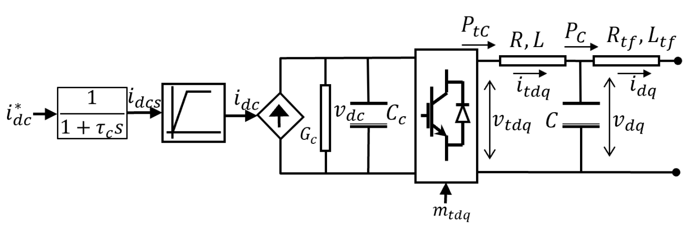

Fig. 1. Circuit diagram of GFC: The dc side is represented as a current source, which mimics the characteristics of a renewable source.

The AC side dynamics of the GFC is represented by the RLC filter as:

$$\dot{i}_{tdq} = -\frac{R}{L} i_{tdq} \pm \omega_c i_{tqd} + \frac{1}{L}(v_{dq} - v_{tdq}) \tag{1}$$

$$\dot{v}_{dq} = \pm \omega_c v_{qd} + \frac{1}{C}(i_{tqd} - i_{dq}) \tag{2}$$

The RLC filter connects the converters to the ac grid through a transformer, whose dynamics are represented by equivalent leakage inductance as:

$$\dot{i}_{dq} = -\frac{R_{tf}}{L_{tf}} i_{dq} \pm \omega_c i_{qd} + \frac{1}{L_{tf}}(v_{bdq} - v_{dq}) \tag{3}$$

where v_{bdq} is grid side voltage at the point of common coupling.

The dc-link voltage dynamics on the dc side of the VSC is modeled as

$$\dot{v}_{dc} = \left(-G_c v_{dc} + i_{dc}^{\max} sat\left(i_{dcs}/i_{dc}^{\max}\right) - P_{tc}/v_{dc}\right)/C_c \tag{4}$$

where, P_{tc} is the converter terminal power on the ac side. In this study, a lossless converter is assumed, therefore, P_{tc} is same as the dc side power. The saturation function is defined as:

$$sat(u) = \begin{cases} u, & \text{if } |u| \le 1 \\ \operatorname{sgn}(u), & \text{otherwise} \end{cases} \tag{5}$$

The dc-link current limit i_{dc}^{max} is determined by factors like the maximum power point (MPP) combined with the renewable's characteristics. It should be noted that the minimum current limit of the GFC is considered as zero, which implies that the GFC does not receive any power from the grid.

To represent the renewable resource, a dependent dc current source is considered, see Fig. 1. The reference input current i_{dc}^* is expressed as [18]

$$i_{dc}^* = k_{dc}(v_{dc}^* - v_{dc}) + G_c v_{dc} + (P_c^* + P_{tc} - P_c)/v_{dc}^* \tag{6}$$

where, v_{dc}^* and P_c^* are the nominal values of the dc voltage and the GFC power, respectively, and k_{dc} is the dc voltage droop coefficient. Rest of the parameters in (6) are self explanatory from Fig. 1. A delay of τ_c is considered for the dc current to replicate the delay associated with a renewable energy source.

B. GFC Controls

The GFC is controlled in a rotating $d-q$ reference frame whose angular frequency ω_c is imposed by the converter using a power-frequency droop as:

$$\dot{\theta}_c = d_{pc}(P_c^* - P_c) = \Delta\omega_c \tag{7}$$

where, θ_c is the angle of the voltage across the capacitor C, see Fig. 1, and $\omega_c = \omega^* + \Delta\omega_c$.

Two loops of inner controls are considered for the VSC, see Fig. 2. The inner current controller PI_i that controls the current through the RL (Fig. 1) series components, and the voltage controller PI_v that controls the voltage across the capacitor C (Fig. 1). The state variables (x_{GFC}) and the input variables (u_{GFC}) of a detailed GFC model are:

$$\begin{aligned} x_{GFC} &= [i_{dcs}\ v_{dc}\ i_{td}\ i_{tq}\ v_d\ v_q\ i_d\ i_q\ \theta_c\ x_v \\ &\quad x_{vd}\ x_{vq}\ x_{id}\ x_{iq}] \\ u_{GFC} &= \left[v_{dq}^*\ v_q^*\ v_{dc}^*\ P_c^*\ \omega^*\right] \end{aligned} \tag{8}$$

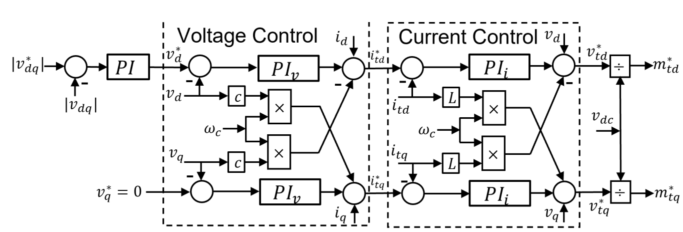

Fig. 2. Schematic of GFC current and voltage controls.

where, x_v, x_{vdq}, and x_{idq} are the state variables of the voltage regulator, voltage controllers (PI_v), and current controllers (PI_i), respectively.
The nonlinear state-space averaged phasor model of a power system with GFC can be derived in the form of the following DAEs:

$$\begin{aligned} \dot{X} &= F\left(X, U, Y\right) \\ 0 &= G\left(X, U, Y\right), \end{aligned} \tag{9}$$

where X, U, and Y are the state-variables, input variables, and algebraic variables, respectively.
Remark I: It can be observed from equations (9) that the power system with GFC model has a nonlinear characteristic with different time-scale dynamics. As these models are used to perform transient stability analysis or design controls for GFC-based system, it is important to know the limitations and characteristics associated with different levels of details in the system models. It is therefore important to derive meaningful reduced order models of the original system. To that end, the singular perturbation analysis make available to derive approximate models to the original system as well as it lightens the high dimensional problem, which is presented next.

III. Singular Perturbation Analysis

Consider a singularly perturbed system of ordinary differential equation [19]:

$$\dot{x} = f\left(t, x, z\right), \;\; x(t_0) = x_0 \tag{10}$$

$$\varepsilon \dot{z} = g\left(t, x, z\right), \; z(t_0) = z_0 \tag{11}$$

where, $\epsilon \in \Re^+$ is a small and typically derived from (dimensionless) normalized time-constants of the system, $x \in \Re^N$, $z \in \Re^n$ are Euclidean space vectors of state variables, and $t \in (t_0, +\infty)$.
We are interested in the faster dynamic states (i.e., z) of dimension n that can be represented as:

$$z = h(t, x) \tag{12}$$

which is an isolated root of $0 = g\left(t, x, z\right)$. Substituting z into (10) gives the reduced order dynamics of the system that can be described as:

$$\dot{x} = f\left(t, x, h(x)\right) \tag{13}$$

Then the boundary layer model can be derived as:

$$dy/d\tau = g\left(t, x, y + h(x)\right) \tag{14}$$

where a change of variable $y = z - h(x)$ is performed to shift the equilibrium of the boundary layer model to the origin, and $\tau = t/\epsilon$ represents a stretched time-scale in which $x(t)$ varies very slowly. Therefore, x is assumed to be a fixed parameter in the boundary layer model.

A. Proposed Approach for the Nonlinear System

Figure 3 shows the process to determine the states to be removed during simplification of the model. Following are the steps of the proposed approach:
Step (1): Develop the nonlinear state-space averaged model of the system that can be expressed in a compact form in

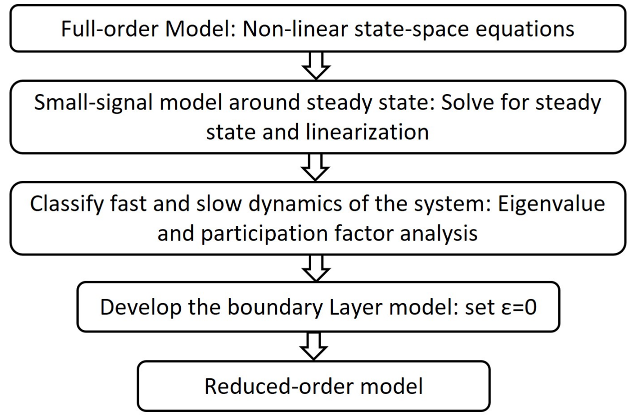

Fig. 3. Steps of the proposed model reduction approach.

equation (9) and solve for the steady state operating conditions ($\bar{x}$, $\bar{u}$).
Step (2): Linearize the nonlinear system around the operating point ($\bar{x}$, $\bar{u}$) and expressed in state-space form as:

$$\Delta \dot{x} = A \Delta x + B \Delta u \tag{15}$$

where, Δx and A are the state-vector and the state-matrix, respectively.
Step (3): Find the eigenvalues (λ) of the system and rank them based on their absolute values from highest to lowest magnitudes and classify them as slow and fast eigenvalues.
Step (4): Perform the participation factor analysis. The right (ψ_i) and the left (ϕ_i) eigen vectors corresponding to the eigenvalues $\lambda_i, \; i = 1, 2, \ldots, n$ that satisfy:

$$A\phi_i = \lambda_i \phi_i, \; \psi_i A = \lambda_i \psi_i \tag{16}$$

Then the participation matrix, P whose elements are calculated as $p_{ki} = \phi_{ki}\psi_{ki}$.
The highest-magnitude eigenvalues are the fastest modes and can be segregated based on a pre-determined threshold. Then participation factor analysis is performed to determine the corresponding states participating in those modes. These states are then removed from the model by replacing the relevant differential equations with algebraic equations.
Step (5): Approximate the differential equations correspond to slowest dynamics states as algebraic equations and derive the reduced order nonlinear model.

IV. Case Studies

A. Test System 1: Single machine and GFC test system

To perform a fundamental analysis, first, a basic model of a power grid with one GFC, an SG, and a load is developed in Matlab/Simulink and is shown in Fig. 4. The detailed model of the GFC discussed in Section II is used here and the SG is represented by a classical model along with a governor model. The load is assumed to be constant power.

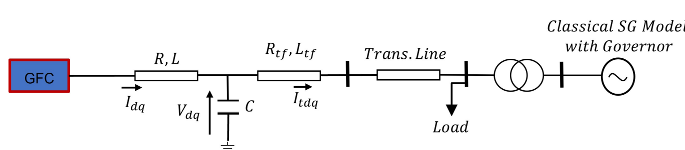

Fig. 4. Test System 1: Single machine and GFC system.

This nonlinear state-space model has 17 states (14 from GFC including transformer and 3 from SG). This model is linearized around the operating point and the eigenvalue analysis is performed (i.e., Steps (2) and (3) of the proposed approach in Section III-A). Then, the participation factor analysis is performed on the linearized system and Table I summarizes participation factors for the first four dominant modes of the system (Step (4)). Table I indicates that the transformer current states participate more in mode 1 and the next three modes have highest participation from states of associated with the RLC filter. Based on this analysis, (by

TABLE I
PARTICIPATION FACTOR ANALYSIS

Pole-pair number	Pole	Dominant states
1	-7.39e+05 $\pm$ 3.71e+02i	i_{tdq}
2	-3.90e+01 $\pm$ 6.44e+04i	v_{dq}
3	-3.77e+01 $\pm$ 6.20e+04i	v_{dq}
4	-2.37e+01 $\pm$ 7.54e+02i	i_{dq}

performing Step (5) of the proposed approach in Section III-A) two types of reduced order models are derived.

- Type 01 Reduced Model: The GFC transformer dynamics are approximated by algebraic equations. There are 15 states in this model.
- Type 02 Reduced Model: In addition to the transformer dynamics, this model approximates all the RLC filter dynamics (i.e., v_{dq}, and i_{dq}) by algebraic equations and the corresponding controls are also ignored (i.e., PI_i, and PI_v in Fig. 2). Moreover, the voltage tracking is assumed to be perfect (i.e., $|v_{dq}| = |v^*_{dq}|$). There are 5 states in this model.

1) Time-Domain Analysis: Dynamic response following a step increase in the load in Fig. 4 is performed for both the reduced models and are compared against the full order model response, is shown in Fig. 5. It can be seen from the Fig. 5 that both reduced-models capture the average performance of the full order model.

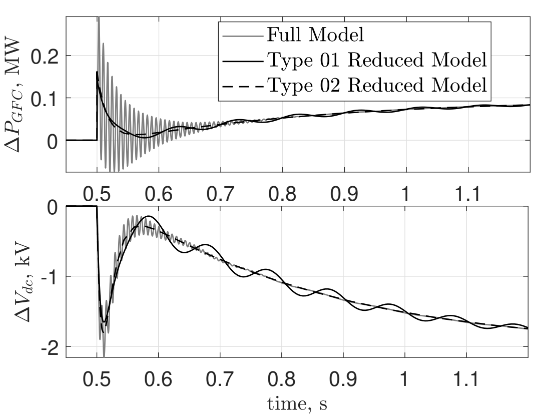

Fig. 5. Test System 1: Comparison of system dynamics following step change in the load.

B. Test System 2: 1-GFC 4-machine system

Our next test system is a modified 2-area 4-machine test system, see Fig. 6 [17]. In this model, all the SGs are represented by the 8^{th}-order subtransient models and are equipped with the IEEE DC1A excitation system and turbine-governors as described in Section II. The detailed model is used for the GFC located at bus 12, see Fig. 6. In the base case, the GFC delivers 350 MW.

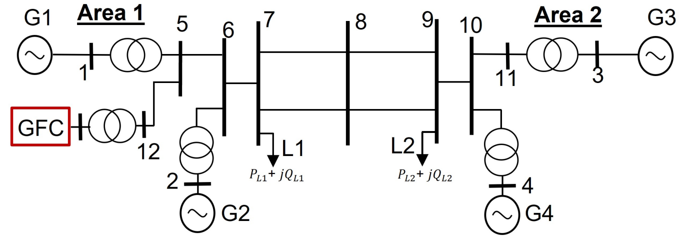

Fig. 6. Test System 2:1-GFC 4-machine system.

The Steps (2)-(4) of the proposed approach in Section III-A are followed here as well, which reveals a similar conclusions for the dominating modes and corresponding states for this test system. Based on these analysis two types reduced order models defined in the Section IV-A are derived.

Remark II: It has been observed from an extensive simulation study that the response from the 'Type 01 Reduced Model' closely matches with that of the full-order model. Due to the space constraints in this paper, we are only reporting case studies where the response of the 'Type 02 Reduced Model' is significantly different compared to that of the full-order model. In each case, the GFC will be tripped if its dc-link voltage falls below a 40% threshold of its rated value.

1) Case 1: In this case, the generator G2 producing 83 MW power at the steady state is tripped in test system shown in Fig. 6 when the load composition is constant power. Figure 7 shows the dynamic responses of the full and reduced (Type 02) -order models following this outage. In can be seen from Fig. 7 that for the full-order model, the dc-link voltage collapses leading to a tripping of the GFC. Moreover, in the full-order model, following the GFC tripping the system experiences an ac voltage instability, see bus 7 voltage in Fig. 7. The result based on the reduced model however shows dc-link voltage dips followed by recovery.

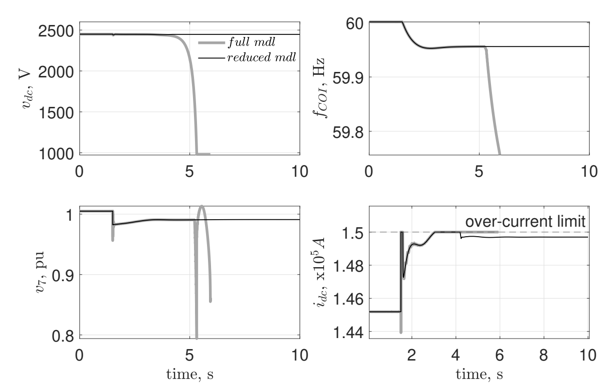

Fig. 7. Case 1: G2 producing 83 MW is tripped when load composition is of constant power. f_{COI}: Centre of inertia frequency.

2) Case 2: In this case, the generator G1 producing 95 MW power is tripped when load composition is of 50%

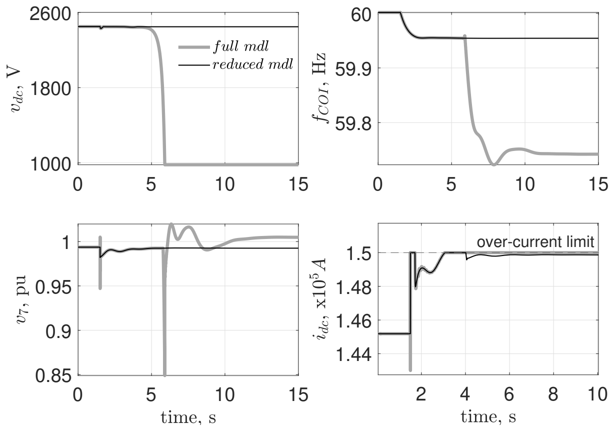

Fig. 8. Case 2: G1 producing 95 MW is tripped when load composition is 50% constant power and 50% constant impedance. f_{COI}: Centre of inertia frequency.

constant power and 50% constant impedance. Here the full model shows a dc-link voltage collapse followed by GFC tripping (Fig. 8), which leads to frequency nadir of 59.72 Hz and steady state frequency deviation as shown in Fig. 8. The GFC tripping leads to significant ac voltage dip but the voltage recovers. On the contrary, the reduced model (Type 02) does not lead to GFC dc-link voltage collapse and its subsequent tripping. Hence the dynamical behavior including the frequency dynamics appear quite different.

3) Case 3: In this case, we trip G4 producing 174 MW power when load composition is of 50% constant power and 50% constant impedance – the dynamic response is shown in Fig. 9. The ac voltage diverges (possibly voltage instability) in the full order model, whereas the reduced model (Type 02) does not show such an impact.

V. Conclusions and Future Work

A singular perturbation analysis-based model reduction approach for nonlinear power system models with GFCs is proposed. The proposed approach have led to two types of reduced order models for GFCs (i.e., Type 01 and Type 02). Using nonlinear time-domain simulations, it was observed that the 'Type 01 Reduced Model' can track the averaged response of the detailed model very closely. Although the 'Type 02 Reduced Model' works fine in most of the time, it was found that in certain scenarios in which a generation loss can lead to non-conservative behavior of reduced models. In those cases, the detailed model show dc or ac voltage instability, whereas the reduced model does not show any instability problems. Our future studies will include GFLCs along with GFCs in the system. Moreover, an analytical approach will be developed to establish modeling adequacy of such complex systems.

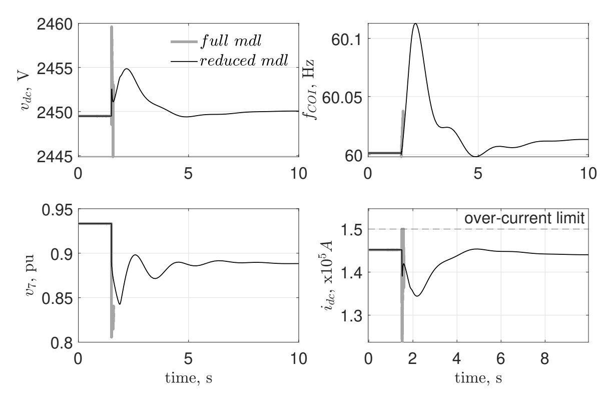

Fig. 9. Case 3: G4 producing 174 MW is tripped when load composition is 50% constant power and 50% constant impedance. f_{COI}: Centre of inertia frequency.

References

[1] N. W. Miller, M. Shao, S. Pajic, and R. D'Aquila, "Western wind and solar integration study phase 3-frequency response and transient stability," *National Renewable Energy Lab.(NREL), USA; GE Energy Management, Schenectady, NY, USA, Tech. Rep.*, 2014.

[2] EirGrid and Soni, "DS3: System Services Review TSO Recommendations," *EirGrid, Tech. Rep*, 2012.

[3] RG-CE System Protection & Dynamics Subgroup, "Frequency stability evaluation criteria for the synchronous zone of continental europe," 2016, eNTSO-E, Tech. Rep.

[4] ERCOT concept paper, "Future ancillary services in ERCOT," 2013, tech. Rep. [Online]. Available: http://www.ercot.com/content/news/presentations/2014/ERCOT_AS_Concept_Paper_Version_1.1_as_of_11-01-13_1445_black.pdf

[5] N. Soni, S. Doolla, and M. C. Chandorkar, "Improvement of transient response in microgrids using virtual inertia," *IEEE Transactions on Power Delivery*, vol. 28, no. 3, pp. 1830–1838, 2013.

[6] H. Bevrani, B. François, and T. Ise, *Microgrid Dynamics and Control*. Wiley, 2017. [Online]. Available: https://books.google.com/books?id=xgETjwEACAAJ

[7] P. Vorobev, P.-H. Huang, M. Al Hosani, J. L. Kirtley, and K. Turitsyn, "A framework for development of universal rules for microgrids stability and control," in *2017 IEEE 56th Annual Conference on Decision and Control (CDC)*, 2017, pp. 5125–5130.

[8] F. Dörfler and F. Bullo, "Synchronization and transient stability in power networks and non-uniform kuramoto oscillators," in *Proceedings of the 2010 American Control Conference*, 2010, pp. 930–937.

[9] A. Tayyebi, F. Dorfler, F. Kupzog, Z. Miletic, and W. Hribernik, "Grid-forming converters - inevitability, control strategies and challenges in future grids application," 2018.

[10] F. Dörfler, M. Chertkov, and F. Bullo, "Synchronization in complex oscillator networks and smart grids," *Proceedings of the National Academy of Sciences*, vol. 110, no. 6, pp. 2005–2010, 2013.

[11] F. Milano, F. Dörfler, G. Hug, D. J. Hill, and G. Verbič, "Foundations and challenges of low-inertia systems (invited paper)," in *2018 Power Systems Computation Conference (PSCC)*, 2018, pp. 1–25.

[12] J. Chow, *Time-Scale Modeling of Dynamic Networks with Applications to Power Systems*. Springer Berlin Heidelberg, 1982.

[13] M. Kabalan, P. Singh, and D. Niebur, "Nonlinear Lyapunov stability analysis of seven models of a dc/ac droop controlled inverter connected to an infinite bus," *IEEE Trans. on Smart Grid*, vol. 10, no. 1, pp. 772–781, 2019.

[14] S. Curi, D. Groß, and F. Dörfler, "Control of low-inertia power grids: A model reduction approach," in *2017 IEEE 56th Annual Conference on Decision and Control (CDC)*, 2017, pp. 5708–5713.

[15] U. Markovic, O. Stanojev, P. Aristidou, E. Vrettos, D. S. Callaway, and G. Hug, "Understanding small-signal stability of low-inertia systems," *IEEE Transactions on Power Systems*, pp. 1–1, 2021.

[16] S. Jafarpour, V. Purba, B. B. Johnson, S. V. Dhople, and F. Bullo, "Singular perturbation and small-signal stability for inverter networks," *IEEE Transactions on Control of Network Systems*, vol. 9, no. 2, pp. 979–992, 2022.

[17] P. Kundur, N. Balu, and M.G. Lauby, *Power System Stability And Control*. New York: McGraw-Hill, 1994.

[18] L. Karunaratne, A. Yogarathnam, N. R. Chaudhuri, and M. Yue, "Grid of near future: Impact on (n-1) contingency analysis in presence of droop-controlled grid-forming converter-interfaced generations," in *2022 IEEE Power and Energy Society General Meeting (presented)*, 2022, pp. 1–5.

[19] H. K. Khalil, *Nonlinear systems; 3rd ed.* Prentice-Hall, 2002.